Received: 5 June 2023 | Revised: 31 October 2023 | Accepted: 16 December 2023

DOI: 10.1002/joc.8348

RESEARCH ARTICLE

International Journal of Climatology RMetS

Unveiling climate change-induced temperature-based hotspots across India through multimodel future analysis from CMIP6

Subharthi Sarkar | **Rajib Maity**

Department of Civil Engineering, Indian Institute of Technology Kharagpur, Kharagpur, India

Correspondence
Rajib Maity, Department of Civil Engineering, Indian Institute of Technology Kharagpur, Kharagpur 721302, West Bengal, India.
Email: rajib@civil.iitkgp.ac.in; rajibmaity@gmail.com

Funding information
Ministry of Earth Science (MoES), Govt. of India, Grant/Award Number: MoES/PAMC/H&C/124/2019-PC-II

Abstract

Global warming and associated climate change impacts have posed major threats to this 21st century's world, especially for developing countries like India, given various socio-economic factors. Considering the extensive spatial diversity of this warming-induced climate changes, suitable region-specific strategies must be adopted to combat its potential implications. Therefore, it becomes crucial to identify the places most exposed to this changing scenario. This study attempts to shed some light towards this by identifying futuristic "temperature-based hotspots" across India through a comprehensive multimodel multiscenario analysis at various spatiotemporal scales. A new and more informative index named "Temperature-based Hotspot Index (THIn)" is proposed for this purpose, which encapsulates various attributes of changing temperature, including its mean, variability and extremes (magnitude, frequency and severity) into a single metric. Bias-corrected future-projected temperature data from 14 state-of-the-art general circulation models (GCMs) have been considered for the analysis, which are participating in the coupled model intercomparison project version 6 (CMIP6). The overall analysis identifies temperature-based hotspots to span predominantly in the west, north and northeast parts of the country. On the other hand, the southern and eastern part of India along the eastern coast are found to be comparatively less exposed to temperature changes in future. Overall, we expect the findings of this study to be beneficial to plan and adopt suitable region-specific management strategies to combat the challenging future in sufficient advance.

KEYWORDS

climate change hotspots, Coupled Model Intercomparison Project version 6 (CMIP6), hotspot map, temperature extremes, Temperature-based Hotspot Index (THIn)

1 | INTRODUCTION

With an aim to combat multifaceted threats imposed by climate change on various aspects of Earth's system, a legally binding international treaty was signed by 196 parties at the 21st conference of the parties (COP 21) in Paris under the united nations framework convention on climate change (UNFCCC)—popularly known as the Paris Agreement (UNFCCC, 2015). This agreement set an internationally agreed-upon target to limit global

warming up to 2°C (preferably 1.5°C) above the pre-industrial baseline by 2100 (Knutti et al., 2016; Roe et al., 2019; Rogelj et al., 2016). However, the long-term record of global surface air temperature indicates that the recent past decade (2011–2020) was already ~1°C warmer than the 1850–1900 baseline (IPCC, 2021). Further studies reveal that the world is on track to breach the temperature target of 1.5°C in the next two decades (Diffenbaugh & Barnes, 2023; Smith et al., 2018). However, the temperature rise will not be uniform across the globe; some parts might experience greater warming than the global average, and some parts lesser. Overall such a level of global warming will greatly accelerate the other changes that are already underway in the climate system, including glacier melting, sea-level rise, ocean heating, and so forth. Most importantly, the global hydrological cycle will be intensified ominously owing to such global warming, resulting in an overall spatiotemporal redistribution of precipitation, and subsequently causing heavy downpours, floods, as well as prolonged droughts in different parts of the world.

However, how this global-scale warming manifests at smaller spatial and temporal scales remains a pivotal concern for the research community in comprehending the changing pattern of climate, thus devising local- or national-scale adaptation and mitigation efforts. Therefore, among this potential spatial heterogeneity of changing patterns of temperature, it is indeed necessary to identify the "climate change-induced temperature-based hotspots," that is, the places with the strongest and most robust aggregated signature of changing temperature. In particular, presenting such hotspots in a map format with strong visual components, known as a "hotspot map," offers significant advantages for academics and policymakers alike. It can convey numerous key information in an easier, captivating and user-friendly way than some regular quantitative analysis. Therefore, identification of these highly responsive regions in the face of climate change serves as a fundamental yet crucial initial step in future risk assessment and adaptation studies.

Towards this, we have considered the entire Indian mainland as our study area. Owing to the confluence of various climatic, geographic and socioeconomic factors (such as strong signals of climate change, diversified geography, high population density, low per capita income, developing economy, etc.), the entire South Asia and notably India have already been identified as one of the critical regions under the climate change (De Souza et al., 2015; Mani et al., 2018). In recent years, unprecedented warming has been reported over several portions of India. In fact, a recent report from India meteorological department (IMD) finds that the annual surface air temperatures is increasing over India at a rate of 0.64°C per 100 years during the period 1901–2022 (IMD, 2022). Such unequivocal warming is resulting in an increase in the frequency, intensity and duration of heat wave incidents across the country (Rohini et al., 2019). For instance, in the year 2022 only, 280 heatwave days have been recorded between March and May, which is the highest in the last 12 years (https://www.downtoearth.org.in/news/climate-change/state-of-india-s-environment-in-figures-india-recorded-280-heat-wave-days-across-16-states-in-2022-most-in-decade-83131, accessed in November 2022). Moreover, in 2022, summer arrived early in India (Aggarwal, 2022; Dash et al., 2022). IMD started to issue high-temperature warnings as early as in March (Basu, 2022). The average maximum temperature recorded in March 2022 was 33.10°C, the highest in the last 122 years, or since the IMD started maintaining its records. Any such temperature-related climate extremes are extremely important due to their strong association with human health and mortality. A recent study by Ray et al. (2021) reports that 17,362 people lost their lives due to high-temperature-related hazards between 1970 and 2019. However, the worrisome fact is that decadal fatality has been steadily increasing lately—the recent past decade (2010–2019) reports almost four times higher deaths (6494 people) as compared to the 1980–1989 period, where 1505 people lost their lives due to heat waves and high-temperature extremes. Another recent study in Lancet evaluates a loss of 167.2 billion potential labour hours due to heatwaves in 2021, resulting in a loss of income equivalent to about 5.4% of India's GDP (Romanello et al., 2022). Further such extreme temperature events have the potential to trigger subsequent meteorological hazards including droughts, floods, high-intensity rainfall, and cyclones (Seneviratne et al., 2012; Trenberth, 2011; Wasko, 2021; Yu et al., 2022)—which in turn may seriously affect the agricultural yield of the country. For a country like India, whose economy primarily depends on rain-fed agriculture (Kishore et al., 2015), it is a massive threat. Therefore, the adverse impacts of the temperature extremes are not only limited to human health and fatalities (Kotharkar & Ghosh, 2021; Pascal et al., 2021; Zhang et al., 2017) but the overall food security, environmental balance and the national economy too can be badly impacted by it (Luan et al., 2019). Keeping all these factors in mind, developing a future temperature-based hotspot map for India is indispensable, which sets the primary objective of this study. We expect it to be immensely beneficial to combat future climate change-induced temperature hazards in key locations well in advance.

Apart from just the identification of hotspots, understanding their underlying mechanism is also very

TABLE 1 Details of GCMs used in this study, participating CMIP6.

S. No.	Model name	Horizontal resolution (latitude × longitude)	Source institute
1	ACCESS-CM2	1.25° × 1.875°	Commonwealth Scientific and Industrial Research Organization, Australia
2	ACCESS-ESM1-5	1.25° × 1.875°	
3	BCC-CSM2-MR	1.1121° × 1.125°	Beijing Climate Center, China
4	CanESM5	2.7673° × 2.8125°	Canadian Centre for Climate Modelling and Analysis, Canada
5	EC-Earth3	0.70° × 0.70°	EC-Earth-Consortium
6	EC-Earth3-Veg	0.70° × 0.70°	
7	CESM2_WACCM	0.9424° × 1.25°	National Center for Atmospheric Research, USA
8	CMCC-ESM2	0.9424° × 1.25°	Fondazione Centro Euro-Mediterraneo sui Cambiamenti Climatici, Italy
9	MPI-ESM1-2-HR	0.935° × 0.9375°	Max Planck Institute for Meteorology, Hamburg, Germany
10	MPI-ESM1-2-LR	1.8652° × 1.8750°	
11	IPSL-CM6A-LR	1.2676° × 2.5°	Institut Pierre Simon Laplace, France
12	IITM	1.9048° × 1.8750°	Indian Institute of Tropical Meteorology Pune, India
13	NorESM2-LM	1.8947° × 2.5°	Norwegian Climate Center (NCC), Oslo, Norway
14	NorESM2-MM	0.9424° × 1.25°	

important. Towards this, we present a detailed and comprehensive spatiotemporal analysis of likely changes in various attributes of temperature over the future. Simulations from multiple general circulation models (GCMs), taking part in the sixth phase of the coupled model intercomparison project (CMIP6) under various emission scenarios are utilized for this purpose after suitably correcting the inherent model bias. Further to understand the potential spatial heterogeneity of the temperature changes, the results are interpreted with respect to seven different regions of India (see section 3 for further details). Overall, we expect the findings of this study, including the future temperature-based hotspot map, will be highly beneficial not only for academic or research purposes, but for decision-making, risk analysis, impact assessments and planning suitable adaptation and mitigation strategies.

2 | DATA USED

The present study employs daily maximum and minimum temperature data from 14 state-of-the-art CMIP6-GCMs under r1i1p1f1[1] initial condition. Selection of those 14 GCMs from CMIP6 was based on their availability under the aforesaid r1i1p1f1 initial condition and three scenarios—historical, SSP245 and SSP585, during the commencement of this study. This most recent version of CMIP, that is, CMIP6 offers significant advancements over previous versions from various perspectives, such as finer horizontal resolution, improved depiction of the synoptic processes, and better agreement with the global energy balance (Supharatid et al., 2021). Eventually, the projections from CMIP6 becomes more reasonable and trustworthy than those of its earlier iterations (Chen et al., 2021; Di Luca et al., 2020; Li et al., 2021; Wang et al., 2021). Therefore, from multiple CMIP6-GCMs, we obtained the temperature data under r1i1p1f1 initial condition, details of which are shown in Table 1 (https://esgf-node.llnl.gov/search/cmip6/ accessed in November 2022). The future data is obtained over 80 years (2021–2100) period, which is further split into two equal parts, viz. near-future period (2021–2060) and far-future period (2061–2100), to capture the temporal changes in the temperature characteristics w.r.t. the base period (1981–2010). Further, for each GCM, two different shared socioeconomic pathways (SSPs), viz., SSP245 and SSP585, are considered to understand two possible pathways of changes in the future. For instance, SSP585 is the most pessimistic scenario associated with strong economic growth, abundant use of fossil fuel resources, rapid technological advances, but no suitable climate policy (Gidden et al., 2019). On the other hand, SSP245 depicts a "middle of the road" scenario with moderate population growth, uneven development and income growth across countries. Thus, a comparison of results obtained between SSP585 and SSP245 will help us to understand

the possible impacts of higher anthropogenic activity and greenhouse gas emissions in the future.

The bias present in this GCM-simulated dataset is corrected w.r.t. a gridded observational dataset from India meteorological department (IMD). This $1.0^\circ \times 1.0^\circ$ dataset was developed by Srivastava et al. (2009) using observed records of daily maximum and minimum temperature data from more than 350 stations across India. This gridded dataset from IMD perfectly captures the spatial diversity of temperature over India and has been successfully used for various hydroclimatic studies in recent times (Mishra et al., 2017; Sharma & Mujumdar, 2017; Singh et al., 2021).

3 | METHODOLOGY

The entire analysis is carried out in three steps in accordance with the study's objectives. First, the raw GCM temperature data from all 14 models are suitably regridded and bias-corrected. In the second stage, this bias-corrected multimodel multiscenario dataset is undergone a thorough spatiotemporal analysis to understand the impact of changing climate on future temperature. Finally, the future-projected temperature-based hotspot map is developed for the country. The following sections explain the aforesaid steps in the methodology in detail.

3.1 | Regridding and bias correction of future-simulated temperature data from GCMs

Bilinear interpolation, a common regridding technique, is used to overcome the disparity between the spatial resolutions of the 14 CMIP6-GCMs (Table 1). The simulated data from all 14 GCMs are regridded to the common resolution of 1.0° latitude $\times$ 1.0° longitude, same as that of IMD data.

Although the GCM outputs are frequently used for various impact assessment studies, they most commonly suffer from the presence of a significant amount of systematic bias due to their coarse resolution or model parameterizations (Ashfaq et al., 2017; Mishra et al., 2014), which in turn limits their applicability for local or regional scale research. Towards this, a widely used bias-correction method, named empirical quantile mapping (EQM), is adopted in this study to correct the bias in GCM-simulated temperature values—both maximum and minimum. Generally in quantile mapping (QM) methods, the aim is to find a suitable statistical transformation function (f) that maps the raw model output to a new distribution such that the resulting distribution matches that of observations (x_{obs}). It can be mathematically expressed as (Piani et al., 2010)

$$x_m^{bc} = f\left(x_m^{raw}\right), \tag{1}$$

where x_m^{raw} is the raw model output and x_m^{bc} is the bias-corrected model output. If the statistical distribution of x_m^{raw} and x_{obs} are known, the Equation (1) can be rewritten as

$$x_m^{bc} = F_{obs}^{-1}\left(F_m^{raw}\left(x_m^{raw}\right)\right), \tag{2}$$

where F_m^{raw} and F_{obs} are the cumulative distribution functions (CDFs) of the raw model output (x_m^{raw}) and observations (x_{obs}), respectively. In the case of EQM, instead of assuming any parametric distributions, empirical CDFs are estimated directly from the data and used in Equation (2). Thus, the method becomes free from any parametric assumption, and hence is expected to yield better results (Gudmundsson et al., 2012).

3.2 | Spatiotemporal analysis of future changes in temperature

Owing to the diverse landscape of India, a two-way decomposition—spatially and temporally, is done in this study to capture and interpret the true changing scenario of temperature in the future across India. Temporally, the entire year is divided into four different seasons: (i) summer (March–April–May), (ii) monsoon (June–July–August–September), (iii) postmonsoon (October–November–December) and (iv) winter (January–February). In India, mostly hot and dry weather prevails during the summer season, with few occurrences of localized heatwave incidents, as well as thunderstorms. It is followed by a 4-month-long monsoon season, which is initiated by the entry of humid southwesterly monsoon wind causing a huge amount of rainfall (almost 70% of the annual rainfall) for most parts of the country. During the postmonsoon season, a different monsoon cycle, known as the northeast or "retreating" monsoon, brings cool, dry and dense air masses to large parts of India. Finally, the cold and dry winter season comes with very less amount of precipitation across the country.

Spatially, we consider seven different regions in India, by grouping its states and union territories (UTs) based on their geographical location, as shown in Figure 1. Table 2 summarizes this regionalisation, for example, the "west" region is predominantly formed by Rajasthan and Gujrat—generally characterized by very hot summer. Likewise, five states—Karnataka, Kerala,

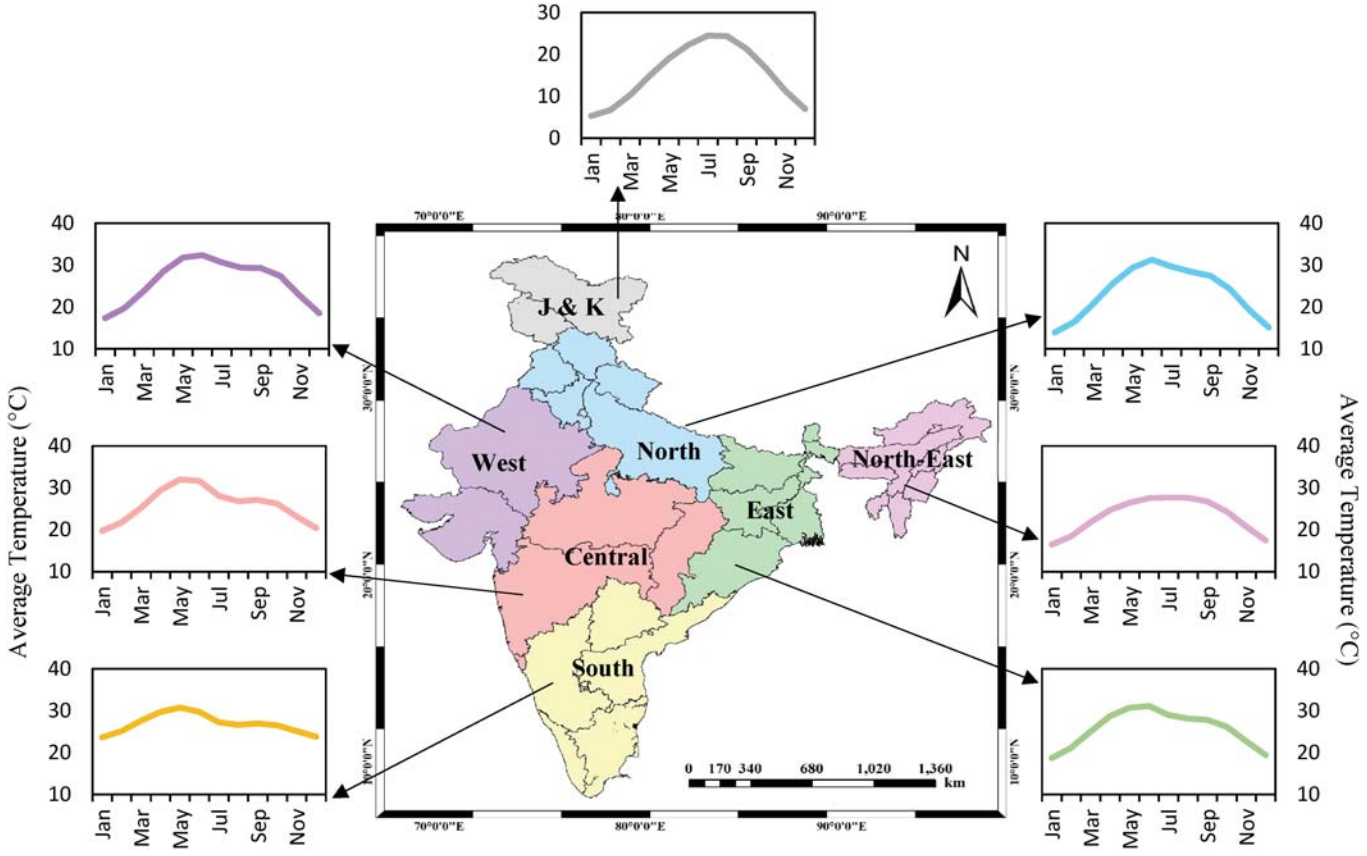

FIGURE 1 Study area map: Entire Indian Mainland and her present states and union territories, grouped into seven different zones based on their geographical locations—West, North, Central, South, East, Northeast and Jammu & Kashmir (J&K). All the regions have different pattern of temperature variation over the months. [Colour figure can be viewed at wileyonlinelibrary.com]

TABLE 2 Details of seven regions of India, considered in this study.

S. No.	Name of the region	States/Union Territories (UTs) in Indian mainland
1	West	Rajasthan, Gujrat, Dadra and Nagar Haveli, and Daman and Diu
2	North	Uttar Pradesh, Delhi, Punjab, Haryana, Chandigarh, Himachal Pradesh
3	Central	Maharashtra, Madhya Pradesh, Goa, Chhattisgarh
4	South	Karnataka, Kerala, Andhra Pradesh, Telangana, Tamil Nadu and Puducherry
5	East	West Bengal, Odisha, Jharkhand, Bihar, Sikkim
6	Northeast	Assam, Meghalaya, Arunachal Pradesh, Nagaland, Manipur, Mizoram, Tripura
7	J&K	Jammu-Kashmir and Ladakh

Andhra Pradesh, Telangana and Tamil Nadu—forms the "south" region, which experiences low variability of temperature throughout the year, with very warm winter. It also has the "J&K" region with the newly formed UTs Jammu-Kashmir and Ladakh in the northernmost part of the country, where the climatology is predominantly cold. Similarly, other regions such as "north," "central," "east" and "northeast" can be identified from Figure 1 or Table 2 with varying pattern of temperature.

Now, using this spatial and temporal decomposition, we perform three different sets of analysis. In the first set of analyses, the expected changes in temperature at annual scale are explored. The likely changes in seasonal variation of temperature over future are investigated in the second set of analyses. And, the third set of analyses is designed to capture the projected changes in extreme temperature over the future. Here, 95th percentile is considered as a measure of extremes. It must be noted here that all the changes are estimated for maximum, minimum and average temperature and expressed in terms of absolute changes (i.e., the changes in magnitude) w.r.t. the base period 1981–2010. Additionally, trend analyses are also performed to identify the places with the statistically significant trend and its magnitude. The Mann–Kendall test at 5% significance level is performed to detect the significant trend, and Sen's slope method (Sen, 1968) is used to evaluate the magnitude of the trend.

3.3 | Identification of temperature-based climate changes hotspots

In this paper, we employ a climate response-based technique to identify the potential "climate change-induced temperature-based hotspots" in the future across India. According to this approach, a hotspot is an area where specific climate variables—in this case, temperature—show particularly pronounced "response" to a particular scenario of global climate change (Sarkar et al., 2023). "Response" in this context refers to the changes in various attributes of temperature between the baseline (1981–2010) and future periods. To this end, we utilize the concept of standard Euclidean distance (SED) to define a new and more informative index, henceforth named as "Temperature-based Hotspot Index (THIn)" which encapsulates the total change in multidimensional temperature characteristics including its mean, variability and extremes. Mathematically, it can be expressed as

$$\mathrm{THIn}=\sqrt{\sum_{i=1}^{N_\Delta}\sum_{j=1}^{N_S}\left(\frac{\delta_{ij}}{\max\left(\left|\delta_{ij}\right|\right)}\right)^2}, \tag{3}$$

where δ_{ij} is the ith temperature change indicator for the jth season at each grid point. Here, we consider totally seven temperature change indicators (thus, $N_\Delta=7$) for four seasons separately: summer, monsoon, postmonsoon and winter (so, $N_S=4$). These seven indicators include (i) change in mean temperature (ΔT), (ii) change in the interannual coefficient of variation of the detrended temperature (ΔT_{var}), (iii) change in the extreme (95th percentile) temperature (ΔT_{ex}), (iv) frequency of hotter seasons, that is, seasons with higher than the maximum temperature in the base period (f_{hot}), (v) increase in average temperature in the hotter seasons w.r.t. the maximum in the base period (ΔT_{fhot}), (vi) frequency of cooler seasons, that is, seasons with lower than the minimum temperature in the base period (f_{cool}), (vii) decrease in average temperature in the cooler seasons w.r.t. the minimum temperature in the base period ($\Delta T_{\mathrm{fcool}}$).

Compared to some other comparable indices used in earlier studies, such as Diffenbaugh and Giorgi (2012) and Turco et al. (2015), this new index THIn takes into account some additional temperature change indicators (δ) such as ΔT_{ex}, ΔT_{fhot} and $\Delta T_{\mathrm{fcool}}$, and hence, presents a more inclusive and informative metric of changing characteristics of temperature. For instance, ΔT_{ex} considers the changes in the level of extreme temperature. On the other hand, although f_{hot} and f_{cool} assess the frequency of hotter or cooler seasons in the future, the severity perspective still remains absent, that is, by what extent the seasons will be hotter or cooler w.r.t. the base period. The present study, therefore, includes ΔT_{fhot} ($\Delta T_{\mathrm{fcool}}$), which denotes a change in average temperature above (below) the maximum (minimum) temperature in the base period. Thus, the magnitude, frequency and severity of extreme temperature all are taken care of by the additional inclusion of these three extra indicators.

Therefore, consideration of all these seven temperature change indicators over four seasons in a year enables to encapsulate all important statistical measures of changing pattern of temperature—mean, variability and extremes. Moreover, in case of extremes, both hot and cold extremes are considered along with its magnitude, frequency and severity of occurrences. Consideration of all these attributes helps us to formulate a comprehensive, inclusive and holistic index THIn to quantify the changing pattern of temperature. However, as expected, different change indicators will have distinct value ranges, which need to be rescaled to a uniform range before summing up to determine THIn, as depicted in Equation (3). This is accomplished by dividing each change indicator by its highest absolute value ($\max|\delta_{\mathrm{ij}}|$) across the study area. In order to make THIn a relative metric of aggregated temperature changes that can be directly compared between any regions within the study area, forcing pathways and future periods, we rescaled each indicator of both the scenarios and periods using the maximum value in the far-future period under the highest forcing (i.e., SSP585) across the study area. Overall considering seven temperature change indicators for four different seasons, we get a total of 28 dimensions at each grid point, which limits the values of THIn between zero and $\sqrt{28}=5.29$. However, it must be noted that similar to other earlier indices, the THIn is also a comparative index, which means a small THIn value does not necessarily imply a small absolute change, but only a small climate response compared to other places within the study area. Moreover, from Equation (3) it is evident that this THIn index is bi-directional, that is, the index cannot differentiate between a place with a strong increase in temperature and a place with a strong decrease in temperature, and, designate them as equally problematic under climate change.

4 | RESULTS AND DISCUSSION

4.1 | Efficacy of EQM method for bias correction

As stated earlier, the present study employs the EQM method to correct the daily-scale GCM-simulated maximum and minimum temperature w.r.t. IMD observed maximum and minimum temperature data over a

common historical period 1961–2014. The efficacy of the EQM technique is examined by considering three temperature-derived statistics for both Tmax and Tmin, viz., (i) mean annual Tmax and Tmin, (ii) mean annual 95th percentile of Tmax and Tmin and (iii) monthly variation of both Tmax and Tmin. Needless to say, consideration of all these variables will be sufficient enough to assess the effectiveness of EQM in correcting bias in the level of mean and extreme temperature, as well as the monthly variation will help to confirm the correctness of the seasonal pattern for both Tmax and Tmin.

The results for mean and extreme in terms of multimodel ensemble (MME) mean are shown in Figure S1, Supporting Information for both mean and extreme (95th percentile) levels of Tmax and Tmin. It can be noticed from the figure that, the GCMs mostly underestimate (cold bias—shades of blue) Tmax in the coastal regions and Himalayan belt, and overestimate (hot bias—shades of red) in the central region. However, in the case of Tmin, GCMs mostly overestimate the coastal and eastern India and underestimate the Himalayan belt, along with the western arid region (panel d). In the case of extremes, the biases—both hot and cold, get even more pronounced w.r.t. the observations, as evident from the figure (2nd and 4th row). The bias-corrected data (panel c) on the other hand, shows a noticeably improved agreement with the observed data, resulting in nearly zero residual bias (panel e) throughout India for both mean and extremes. Thus the efficacy of the EQM method in debiasing the raw Tmax and Tmin data from the GCM simulation is established. Correspondingly, Figure S2 in Supporting Information depicts remarkably good conformity between the observed (black) and bias-corrected (blue) monthly variation of Tmax and Tmin, averaged over the entire Indian mainland. On the contrary, the performance of multimodel raw GCM output (red) is quite poor in capturing the month-wise variation of temperature over India, even with a higher uncertainty range.

Additionally, we assessed the performance of each individual model after bias correction, using root mean square error (RMSE) and percentage absolute bias (PBIAS) relative to the IMD observed Tmax data for the common historical period (1961–2014). The results are summarized in Figure S3, presenting both region-wise averages and an all-India average across all 14 models. Overall, after bias correction, all models exhibited reasonably good performance, with RMSE values below 0.9°C and PBIAS values mostly less than 3% across all regions. At all-India level, GCMs like BCC-CSM2-MR and EC-Earth3-Veg demonstrated the best performance. In addition, models such as ACCESS-CM2, ACCESS-ESM1-5, EC-Earth3, MPI-ESM1-2-HR and IITM also showed good agreement with the observational data. On the other hand, models like INM-CM4-8 and INM-CM5-0 had relatively poorer performance. Region-wise analysis revealed consistently good model performance over the central, south, east and northeast regions of India, while the performance in the J&K region was comparatively poorer across most of the models. Nevertheless, the multimodel average performance was notably strong, further affirming the effectiveness of the EQM bias-correction method and hence it has been used to effectively debias the raw GCM-simulated future temperature data from 14 CMIP6-GCMs, and used for subsequent analysis.

4.2 | Future-projected changes in temperature across India

In this section, we present and discuss the expected future changes in mean and extreme (95th percentile) levels of maximum, minimum and average temperature across India and its various regions. The results are suitably interpreted at annual scale, as well as across four different seasons (viz., summer, monsoon, postmonsoon, winter) through an aggregated multimodel analysis using bias-corrected CMIP6-GCMs. The summary of this assessment for all seasons, two emission scenarios (SSP 245 and 585) and two future periods (near- and far-future periods) are provided both visually and quantitatively in this section. Spatial variation of the expected changes and underlying trends are presented in map format, along with region-wise bar plots and time-series plots of the multimodel ensemble (MME) means. The quantitative outcome of this analysis in terms of MME mean changes and its 95% confidence interval, averaged over the entire India and its seven regions are also provided in tabular format.

4.2.1 | Changes in temperature at the annual scale

Overall, an increasing annual average temperature is projected across the country under both the future scenarios, as can be seen from Figure 2 (first row)—which gets further stronger in the far-future period under the highest forcing scenario. Although this increasing pattern is true for the entire Indian mainland, it is particularly prominent in the northern and northwestern parts of the country. This continuously rising average temperature can also be visualized and confirmed in Figure 3, which depicts the all-India averaged contiguous time series and associated model uncertainty (95% confidence interval). Quantitatively the results are summarized in Table 3, which depicts that on average the Indian mainland is

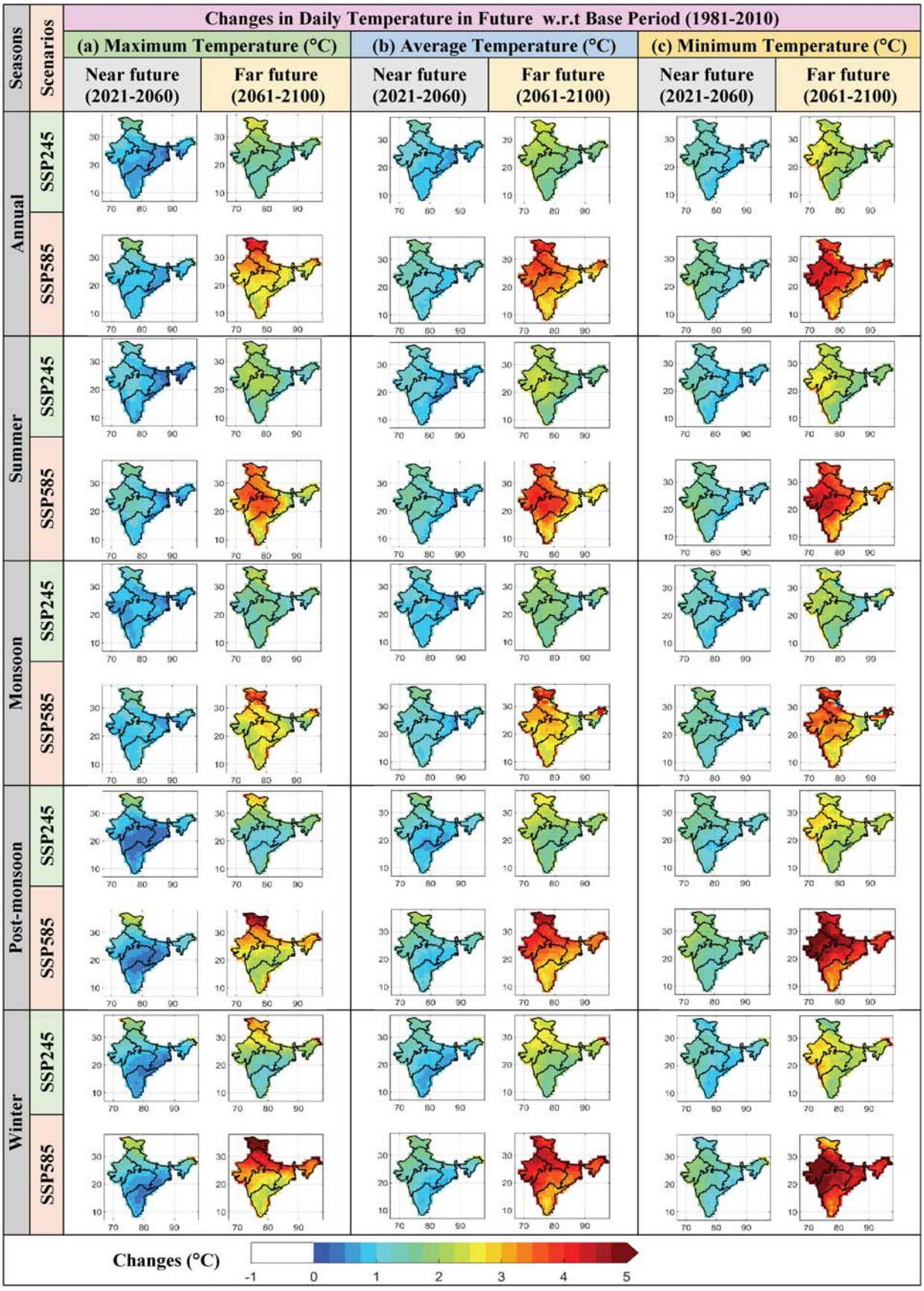

FIGURE 2 MME mean projected changes in daily Tmax, Tavg and Tmin across different seasons over near- and far-future following two scenarios—SSP245 and SSP585. [Colour figure can be viewed at wileyonlinelibrary.com]

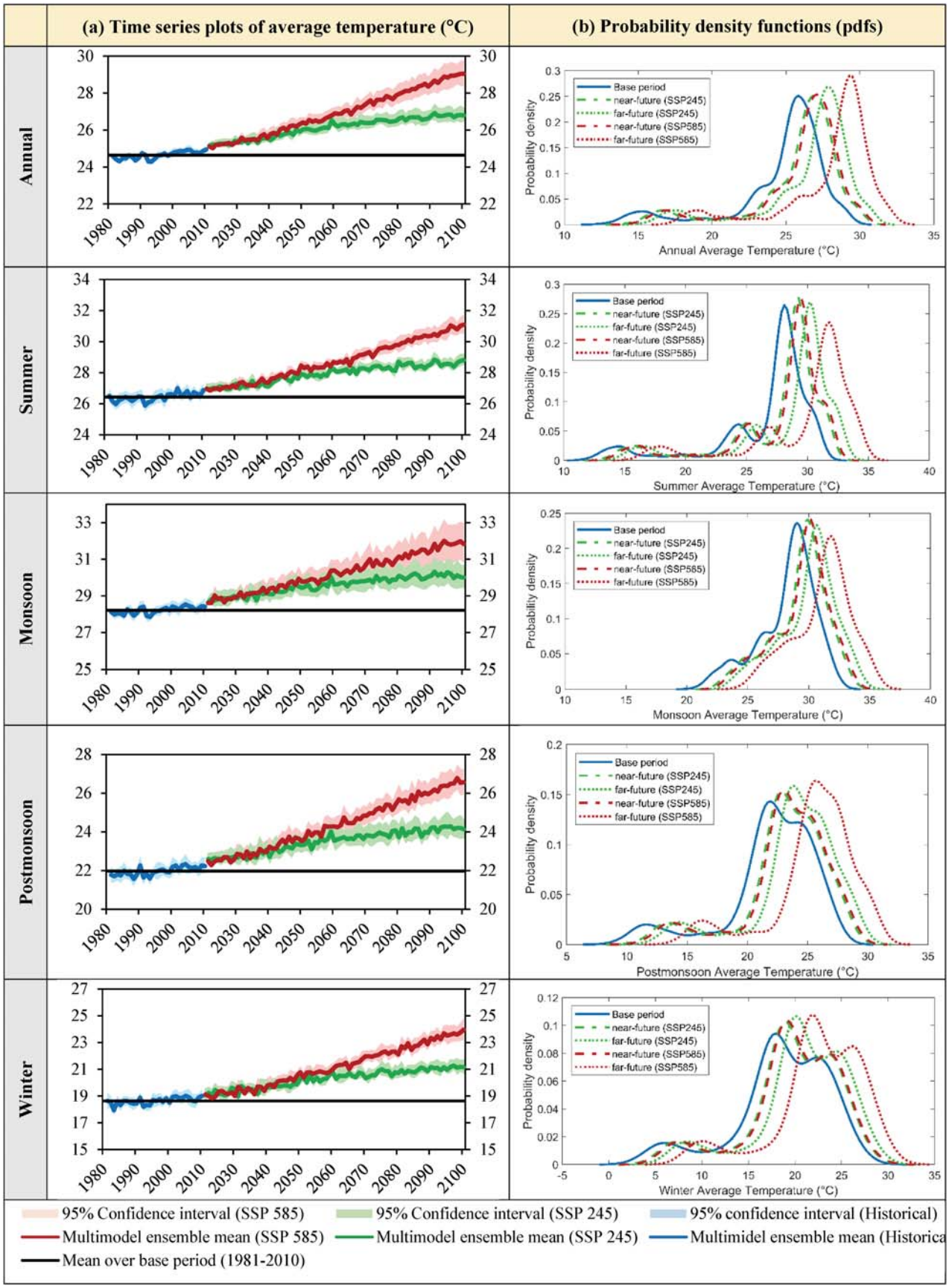

FIGURE 3 (a) MME mean annual time series plots of seasonal average temperature and its 95% confidence interval, averaged across India over 1981–2100, and (b) underlying pdfs over near- and far-future period, following two scenarios considering all grid points across India. [Colour figure can be viewed at wileyonlinelibrary.com]

TABLE 3 MME mean changes and trend in seasonal temperature in future, averaged over entire India along with its 95% confidence interval following two different scenarios. Each cell in the table shows maximum, average and minimum temperature from top to bottom in order. [Colour table can be viewed at wileyonlinelibrary.com]

Scenario and Time Frame wise alteration		Temperature Index over different Time Frame (Annual/Season) along with mean value over base period (°C)									
		Annual (Mean over base period)		Summer		Monsoon		Postmonsoon		Winter	
		Tmax (30.62) Tavg (24.64) Tmin (18.67)		Tmax (33.27) Tavg (26.43) Tmin (19.59)		Tmax (32.88) Tavg (28.21) Tmin (23.55)		Tmax (28.18) Tavg (21.97) Tmin (15.76)		Tmax (25.61) Tavg (18.64) Tmin (11.66)	
		Change and Trend with respect to base period									
Scenario	Time period	Changes (°C)	Trend (°C /decade)	Changes (°C)	Trend (°C /decade)	Changes (°C)	Trend (°C /decade)	Changes (°C)	Trend (°C /decade)	Changes (°C)	Trend (°C /decade)
SSP 245	Near future	0.85 ± 0.23	0.27 ± 0.07	0.86 ± 0.27	0.28 ± 0.08	0.83 ± 0.30	0.25 ± 0.10	0.79 ± 0.26	0.25 ± 0.10	0.98 ± 0.29	0.33 ± 0.11
		1.02 ± 0.24	0.30 ± 0.07	1.00 ± 0.27	0.30 ± 0.08	0.98 ± 0.28	0.25 ± 0.08	1.07 ± 0.25	0.30 ± 0.09	1.09 ± 0.28	0.36 ± 0.10
		1.19 ± 0.26	0.32 ± 0.07	1.13 ± 0.28	0.32 ± 0.08	1.12 ± 0.29	0.26 ± 0.08	1.34 ± 0.30	0.35 ± 0.09	1.19 ± 0.32	0.38 ± 0.10
	Far future	1.68 ± 0.34	0.14 ± 0.06	1.75 ± 0.37	0.14 ± 0.07	1.57 ± 0.49	0.13 ± 0.09	1.57 ± 0.35	0.14 ± 0.09	1.98 ± 0.35	0.18 ± 0.11
		1.92 ± 0.36	0.15 ± 0.05	1.95 ± 0.36	0.15 ± 0.07	1.74 ± 0.47	0.13 ± 0.07	1.97 ± 0.36	0.16 ± 0.07	2.18 ± 0.36	0.20 ± 0.10
		2.16 ± 0.4	0.16 ± 0.05	2.16 ± 0.39	0.17 ± 0.07	1.9 ± 0.49	0.13 ± 0.06	2.37 ± 0.43	0.17 ± 0.08	2.38 ± 0.46	0.23 ± 0.10
SSP 585	Near future	1.01 ± 0.28	0.42 ± 0.08	1.06 ± 0.35	0.42 ± 0.11	1.01 ± 0.36	0.38 ± 0.13	0.92 ± 0.3	0.43 ± 0.09	1.08 ± 0.34	0.48 ± 0.12
		1.23 ± 0.29	0.46 ± 0.08	1.22 ± 0.34	0.46 ± 0.09	1.18 ± 0.33	0.39 ± 0.12	1.27 ± 0.29	0.50 ± 0.08	1.26 ± 0.33	0.54 ± 0.11
		1.44 ± 0.31	0.50 ± 0.08	1.38 ± 0.35	0.51 ± 0.08	1.36 ± 0.34	0.40 ± 0.12	1.62 ± 0.35	0.57 ± 0.09	1.44 ± 0.38	0.60 ± 0.13
	Far future	2.91 ± 0.53	0.53 ± 0.11	3.05 ± 0.64	0.59 ± 0.13	2.62 ± 0.76	0.44 ± 0.15	2.84 ± 0.49	0.52 ± 0.12	3.39 ± 0.51	0.62 ± 0.16
		3.34 ± 0.56	0.58 ± 0.11	3.40 ± 0.61	0.64 ± 0.12	2.89 ± 0.74	0.47 ± 0.14	3.54 ± 0.50	0.61 ± 0.11	3.87 ± 0.54	0.69 ± 0.17
		3.78 ± 0.63	0.64 ± 0.12	3.75 ± 0.64	0.68 ± 0.12	3.17 ± 0.81	0.49 ± 0.15	4.24 ± 0.63	0.70 ± 0.13	4.36 ± 0.67	0.76 ± 0.20

expected to be warmer by 3.34 ± 0.56°C in the far-future period (2061–2100) following SSP585, relative to the 1981–2010 baseline. To be specific, the last decade (2091–2100) will be hotter by more than 4°C under the highest forcing scenario—which is a really alarming figure. Similar results have been reported in a recent study by Mishra et al. (2020), where a different set of GCMs were used—thereby ensuring robustness of the warming projections. Although the degree of such widespread warming is comparatively lesser under the middle-of-the-road scenario SSP245, still it projects a 1.92 ± 0.36°C warmer future over the country w.r.t. to 1981–2010—which is definitely higher than the target set by Paris Agreement. Unlike SSP585, the annual average temperature does not show a continuously steep increase throughout the century under SSP245, rather it apparently stabilizes around the 2060s (see Figure 3). Moreover, the intermodel uncertainty is comparatively narrower in the case of SSP245. However, irrespective of the forcing scenario, the increase in Tavg is mostly contributed by the Tmin, as can be seen from Figure 5. Although the Tmax is also increasing, but its degree of increase is comparatively lesser than that of Tmin. For instance, when the All-India average increase in Tmin is 3.78°C in the far-future period (SSP585), the same for Tmax is 2.91°C—approximately 1° lesser. This observation holds true for all seven regions, except the J&K region in the north (not shown visually), where the climatology is predominantly cold with hilly terrain.

Even though entire India is showing a warmer future, the degree of warming is not uniform across the regions, as can be seen from Figure 4. The maximum increase in average temperature (>4°C in far-future period under SSP585) is projected in J&K region—the northernmost part of India. Apart from that, the climatologically hotter regions like the west and north region also show a considerable amount of increase in annual Tavg. On the contrary, the southern and eastern sides of India exhibit a comparatively lesser extent of increase. Notably, Srivastava et al. (2017), although based on observational data, has previously identified these same regions in India to have experienced the most substantial temperature increases, thereby suggesting a continuity of the warming trend from the past into the future with a similar or potentially even higher rate of increase. Likewise, Basha et al. (2017) also reports a widespread warming across the country based on multimodel CMIP5 projections through future. Moreover, the increase in temperature gets more prominent with the passage of time and particularly under the higher forcing scenario. Detailed estimates regarding future changes for all regions can be found in Table S1 and Figures S4 and S5.

The results of trend analysis (Figure S6) also reveals a few important insights about changing temperature pattern across the country. The all-India average trend in annual Tavg in the near-future period is expected to be $0.3 \pm 0.07^{\circ}C \cdot decade^{-1}$ following the SSP245 scenario from this multimodel analysis. The same following SSP585 is expectedly higher, that is, $0.46 \pm 0.08^{\circ}C \cdot decade^{-1}$ over the country. However, in the far future, the trend nearly halves ($0.15 \pm 0.05^{\circ}C \cdot decade^{-1}$) under the SSP245 scenario, owing to the underlying assumptions of timely climatic protection measures under this scenario. In contrast, the trend gets even stronger in the far-future period, that is, $0.58 \pm 0.11^{\circ}C \cdot decade^{-1}$ under the most pessimistic scenario SSP585, indicating a potential linkage to increased anthropogenic activities. As expected, the trend is not uniform across the country, as can be seen from Figure S7 in Supplementary Information. Along with the J&K portion, it is most pronounced in the west, north and central parts of the country. Comparatively the trend is lesser in the southern peninsula, the eastern and northeastern parts of India. Similar to our earlier observation, here also the trend in annual Tmin is always higher than that in annual Tmax for the entire Indian mainland, except the J&K region.

4.2.2 | Changes in temperature at seasonal scale

The next question arises, how the change in annual temperature is distributed across four seasons—summer, monsoon, postmonsoon and winter, in a year. Towards this, a detailed season-specific projection of temperature is also done and the results are presented in Figures 2 and 4, in terms of spatial distribution plots and bar plots showing region-wise MME means. Overall we find that this warming pattern persists more-or-less evenly over the seasons. However, the contribution from winter remains maximum for most parts of the country, followed by the postmonsoon season. Whereas, the contribution from the monsoon season remains the least (Figure 5). For instance, the average winter temperature all over India is projected to increase by 3.87 ± 0.54°C in the far-future period under SSP585. The same for postmonsoon is 3.54 ± 0.5°C, followed by summer where a warming of 3.40 ± 0.61°C is expected, and lastly the least increase, although substantial enough, is found for monsoon, that is, 2.89 ± 0.74°C. Interestingly, the intermodel uncertainty range is highest in case of the monsoon session, which is also evident from the time series plots (Figure 3). An analogous finding of least changes in monsoon temperature is also reported by Salunke et al. (2023) in a recent study, which utilizes data

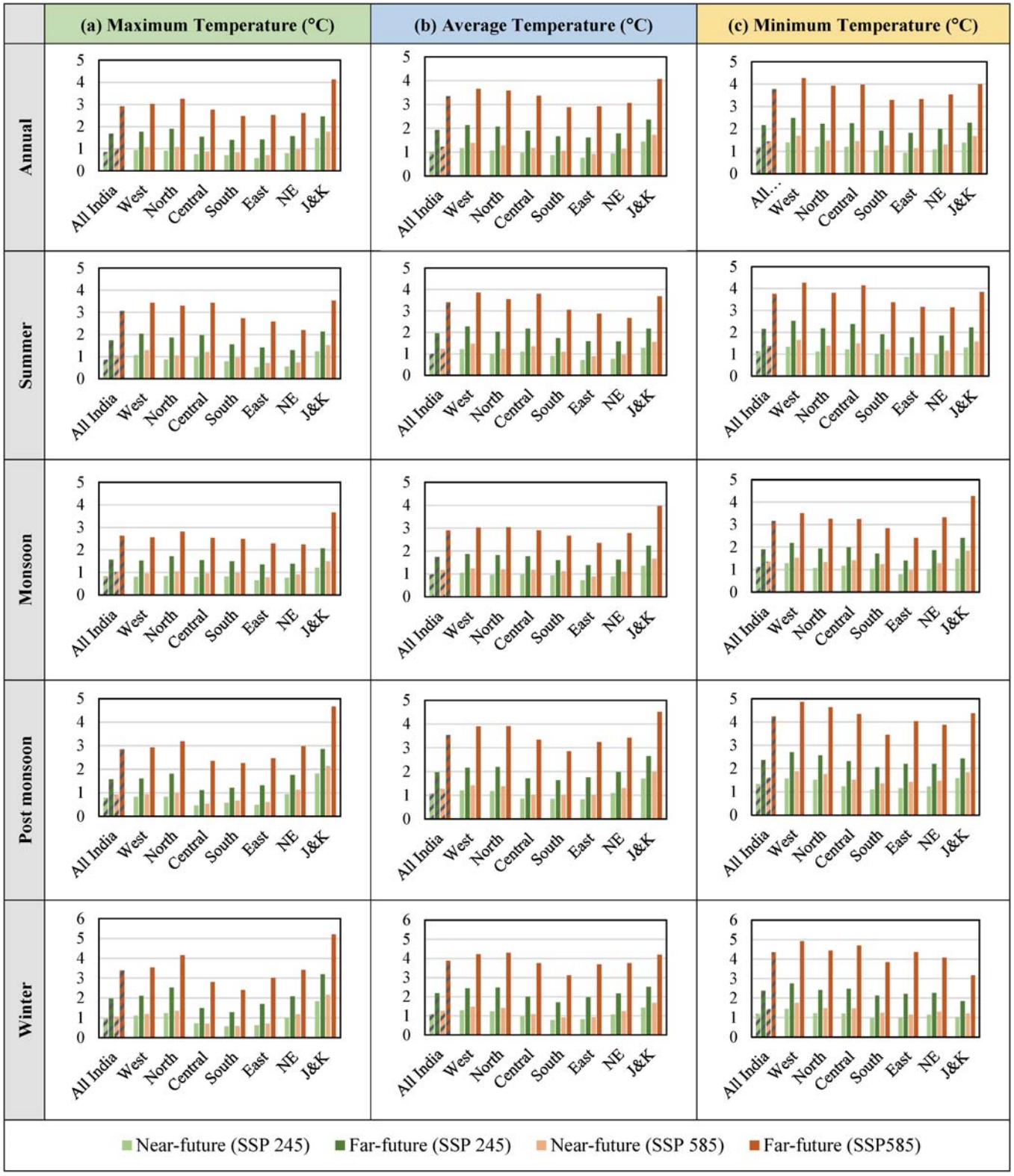

FIGURE 4 HPZ-wise MME mean changes in (a) maximum, (b) average and (c) minimum temperature across different seasons over future following two scenarios. [Colour figure can be viewed at wileyonlinelibrary.com]

from a different source, namely, the national aeronautics and space administration (NASA) earth exchange global daily downscaled projections (NEX-GDDP). Moreover from Figure 3, we can observe a clear future shift in the underlying probability density functions (pdfs) of Tavg over different seasons. These pdfs are developed

FIGURE 5 Seasonal comparison of future MME mean changes in maximum, minimum and average temperature following (a) SSP245 and (b) SSP585 scenario. For both the cases, highest contribution can be seen from winter, and lowest from monsoon season. [Colour figure can be viewed at wileyonlinelibrary.com]

considering all the grid points across India, and hence depicts the spatial distribution of temperature over the country. As expected from our earlier outcome, the shift becomes more prominent under the SSP585 scenario and far-future period. Another interesting observation from these plots are, unlike the summer and monsoon season, the pdf for postmonsoon, particularly for winter season is bimodal in nature. This arises due to relatively diverse spatial distribution of winter temperature across India—where the most part in northern half experiences a winter temperature around 18°C, an almost equally significant part in southern half experiences a comparatively higher temperature around 22°C in winter. On the other hand, except the J&K region, the summer and monsoon temperature varies over a smaller range, resulting in a single-mode distribution. This can be further confirmed form Figures S4 and S5, where fairly higher variability (spatial) can be seen for winter and postmonsoon temperature, as compared to summer or monsoon temperature among the regions.

In general, the observations of warmer winter prevail for all regions of India, except the J&K portion, where postmonsoon session shows the highest warming, followed by winter. The general spatial pattern of the warming is also fairly similar across the seasons. The maximum amount of increase is projected mostly in the northern part of the country, spanning from north-western states like Gujrat and Rajasthan to north-central India and the sub-Himalayan belt, in other words the west and north regions of India. On the other hand, the southern and eastern part of India along the eastern coast consistently shows comparatively lesser warming than the rest of the country. As expected, a similar spatio-temporal pattern is also revealed by the trend analysis over the seasons—depicting a higher trend in winter and across the west, north and J&K regions of India. For instance, when the winter Tavg is showing a trend of 0.36 (0.54) °C·decade^{-1} following SSP245 (585), the same for monsoon is only 0.25 (0.39) °C·decade^{-1} in the near-future period.

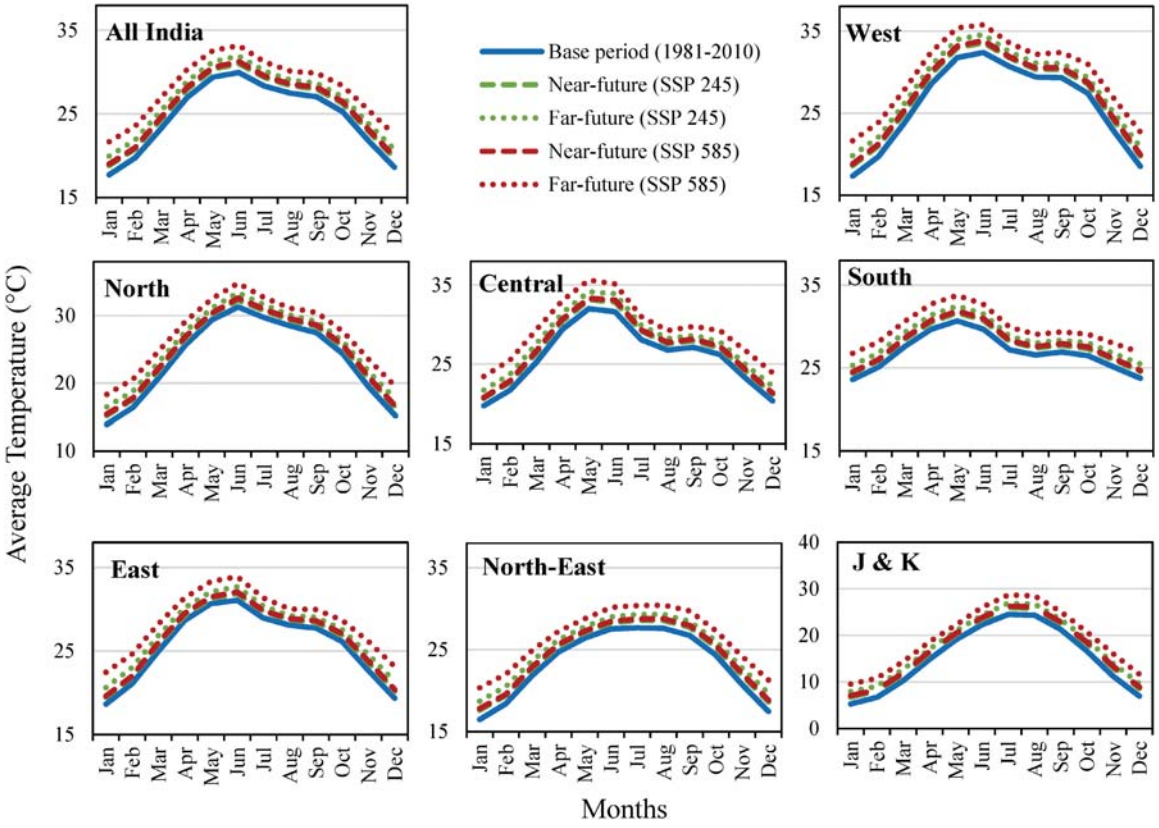

FIGURE 6 MME mean changes in monthly variation of average temperature, averaged across entire India and its seven HPZs over future following two scenarios. [Colour figure can be viewed at wileyonlinelibrary.com]

The seasonal variation of increased temperature is also reflected in Figure 6, which shows the MME mean monthly cycle of average temperature over future periods across India and its regions following two scenarios. This figures nicely depicts the diverse pattern of temperature variation over different regions of India. For some regions, single-peak variation of monthly temperature can be visible with peak around the summer/monsoon season, for example, north, northeast and J&K regions. Additionally, another minor peak around postmonsoon can also be visible for some regions such as south and central India. Preserving this general pattern of temperature variation, a common observation from all the plots, is the unequivocal warming over all months, which gets more intense with time, and under the higher forcing scenario.

4.2.3 | Changes in the 95th percentile (extreme) of average temperature

Similar to the changes in mean levels of Tmax, Tavg and Tmin, detailed analysis is carried out for extreme levels as well. Here, only the 95th percentile of Tmax, Tavg and Tmin is considered as the measure of extreme temperature. Quantitative outcome of the analysis at annual scale is presented in Table S2. Overall it is observed that the increase in extreme temperature will be almost similar to or even stronger than that of mean temperature. For instance, the 95th percentile of annual Tavg is expected to increase by 3.56 ± 0.83°C in the far-future period (SSP585), whereas the same for mean annual Tavg is 3.34 ± 0.56°C. However, the spatial distribution of changes broadly remains similar to that of the mean, that is, a comparatively higher level of increase over northern and western regions, and a lower level of increase in eastern, northeastern and southern India. In the case of extremes also, the contribution from Tmin is higher than Tmax towards overall changes in Tavg, except the J&K region, the northernmost part of the country. However, the seasonal contribution of changes in extreme temperature is a bit different from the mean temperature. At the all-India level, although the contribution from winter remains highest, the contribution from monsoon is almost at par with winter, which was least in the case of mean temperature. This can be explained by the high uncertainty band of the future projection of monsoon Tavg (Figure 3). Similar observations hold for other regions as well.

Overall in a nutshell, the extreme temperature over all the seasons is projected to increase across India at an

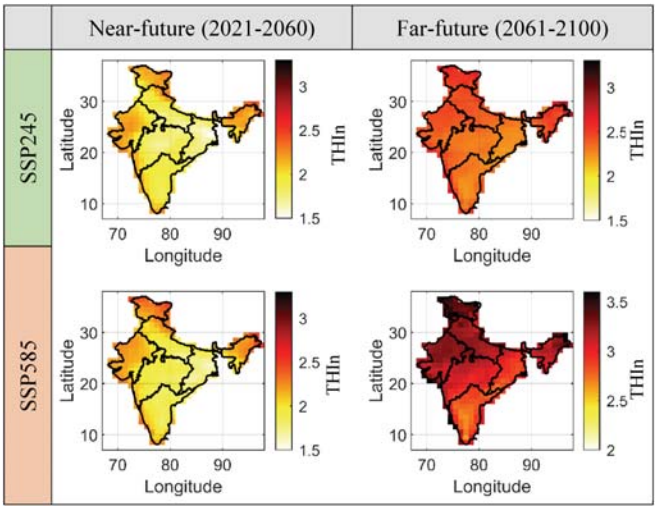

FIGURE 7 Temporal evolution of temperature-based climate changes hotspots across India over future following two scenarios. [Colour figure can be viewed at wileyonlinelibrary.com]

almost similar rate as of mean or sometimes even more pronounced rate, which is definitely a bigger point of concern due to its direct association with heatwaves and other related hazards. For instance, a recent study by Nandi and Swain (2022) has indicated an escalation in the frequency and duration of heatwaves in three densely populated cities in southern India, which can be ascribed to the projected rise in extreme temperatures. Similarly, findings by Rao et al. (2023) have revealed an upward trend in various heatwave attributes, predominantly in India's northwest, central and south peninsular regions—precisely where our present study also anticipates increased extreme temperature conditions. Therefore along with the changes in mean temperature, the changes in extreme temperature holds paramount significance due to their manifold direct and indirect consequences.

4.3 | Temperature-based climate changes hotspots across India over future

As stated in section 3.3, seven temperature change indicators are assessed across the country and rescaled for each of the 14 CMIP6-GCMs for all four seasons. The MME mean is then calculated, followed by the determination of THIn throughout the future periods following two forcing scenarios. The final result is shown in Figure 7 in the form of the spatial distribution of THIn or in other words, future temperature change exposure or susceptibility maps over near- and far-future periods, under SSP245 and SSP585. The places with high values of THIn indicate high exposure to temperature changes and vice versa. Thus the dominant changing pattern in temperature with high values of THIn appears in the northwest, north-central and northeast parts of the country towards EOC under both scenarios. The western coast of India, located on the windward side of the Western Ghats, is also showing substantially high values of THIn. On the other hand, eastern and southern part of the country, particularly along the eastern/Coromandel coast, show comparatively lesser exposure to temperature changes. However, all these less exposed places also tends to exhibit an increase in THIn over time, indicating increasing exposure through the future.

In general, an increase in THIn values is projected across the country with the passage of time and under the worst emission scenario SSP585—very similar to our earlier observations on changes in annual or seasonal temperature. Therefore, considering the THIn map over the far-future period and SSP585, the temperature-based climate change hotspots are identified over India. To this end, firstly a nonparametric Kernel pdf of THIn is developed for all grid points across India for the far-future period (2061–2100) and SSP585 scenario. Then the area under the pdf is split into four different parts based on 25th, 50th and 75th percentile of THIn values (as shown in Figure 8c), and accordingly the entire India mainland is categorized into four susceptibility zones of varying susceptibility—(i) severely susceptible zone (red zone): $THIn \geq THIn_{75}$, (ii) highly susceptible zone (orange zone): $THIn_{50} \leq THIn < THIn_{75}$, (iii) moderately susceptible zone (yellow zone): $THIn_{25} \leq THIn < THIn_{50}$, and (iv) less susceptible zone (green zone): $THIn < THIn_{25}$. Out of these four zones, the first two zones (red and orange zones) are collectively identified as "temperature-based climate change hotspots" in this study. The finally obtained zoned hotspot map is shown in Figure 8b. Further analysis on the spatial distribution of these hotspots across seven regions of India, as shown in Figure 8e, reveals that the J&K region have the maximum (100%) spatial extent of hotspots, followed by west and north regions. However, it is worthwhile to mention here that, the J&K portion is predominantly a cold region. Thus, even if it is highly exposed to changing climate, the projected temperature in absolute terms will be substantially lesser than the climatologically warmer regions like west and north India, where more than three-fourth part area is exposed to high to severe changes in temperature over the future—a really alarming figure. Likewise more than 50% area of northeast India is also identified as temperature change hotspots in the future. On the other hand, expectedly, the south, east and central regions has the least share of hotspots.

Further state-wise analysis (Figure 9) reveals that, along with the UTs—Jammu-Kashmir and Ladakh, the

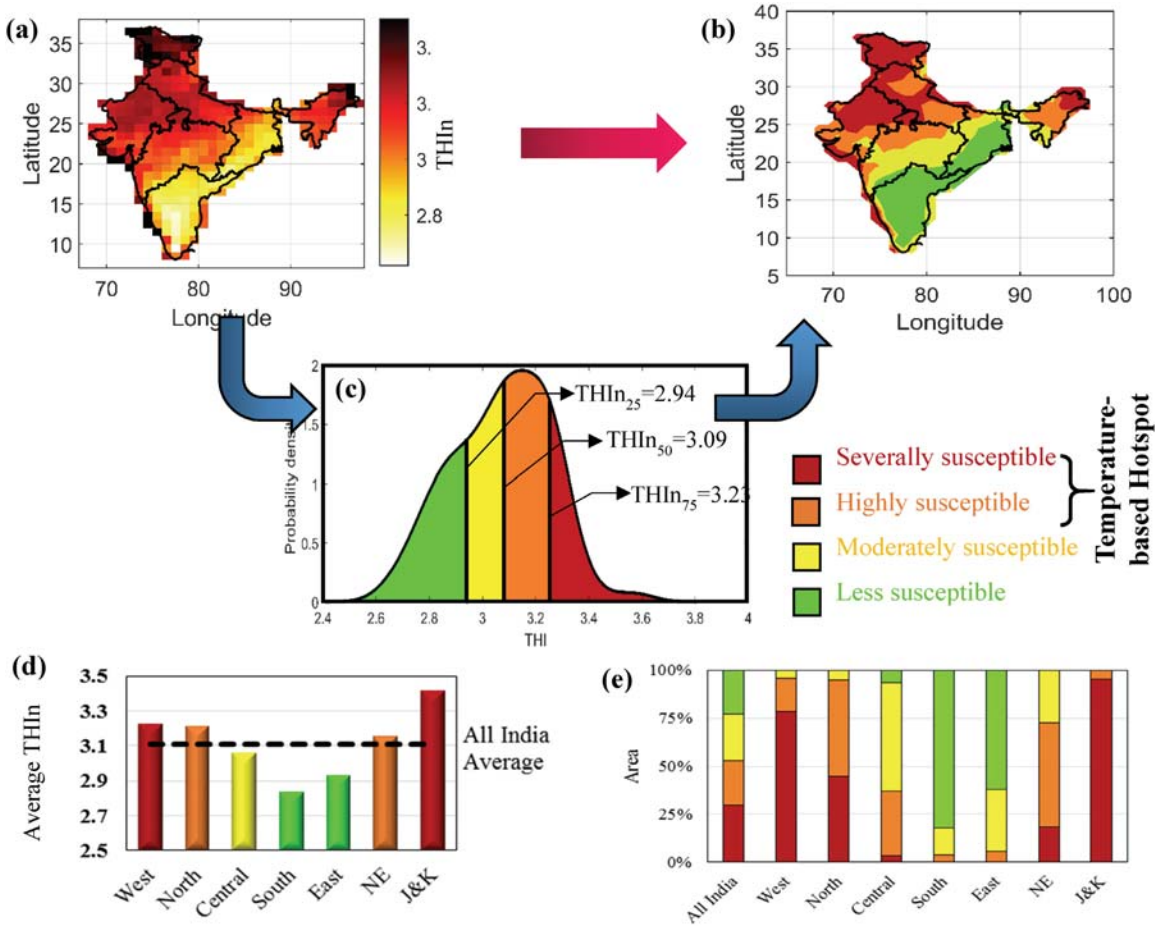

FIGURE 8 Development of temperature changes hotspot map for India in far-future under SSP585. (a) Actual spatial distribution of THIn in far-future under SSP585, (b) transformed hotspot map having four zones, using (c) the pdf of THIn across India. (c) Average values of THIn across HPZs and (d) % of spatial extent under all four colour zones across HPZs. [Colour figure can be viewed at wileyonlinelibrary.com]

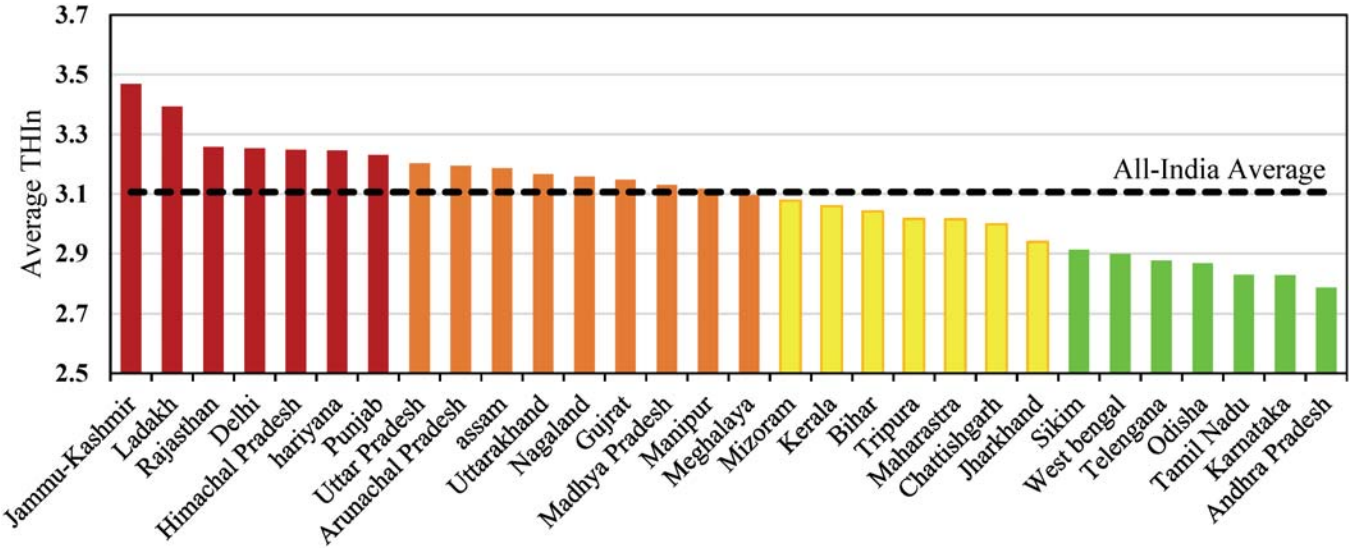

FIGURE 9 State-wise average THIn values across India, arranged in decreasing order of magnitudes. [Colour figure can be viewed at wileyonlinelibrary.com]

northern and western states like Gujrat, Rajasthan, Delhi, Punjab, Haryana, Uttar Pradesh, and northeastern states like Arunachal Pradesh show high values of spatially averaged THIn indicating a substantial degree of temperature changes in the future. On the other hand, eastern and southern states such as West Bengal, Odisha, Andhra Pradesh and Tamil Nadu show comparatively lower values of THIn, depicting a comparatively lesser exposure to temperature changes.

Although the hotspot patterns appear to be robust under various emission scenarios, the results are particularly prone to some sources of uncertainty. For example, the number of GCMs and their realizations considered in the analysis may not be sufficient to capture the full range of uncertainty from the perspective of global climate sensitivity and regional response to global warming, despite using state-of-the-art CMIP6-GCM (Taylor et al., 2012). Thus even when the MME mean is taken into account, the final outcomes may be sensitive to the number of models and their realizations considered. Regardless, the broad implications of this study's findings cannot be ignored in terms of future preparedness and policy formulation.

5 | SUMMERY AND CONCLUSIONS

A new and more inclusive index named Temperature based Hotspot Index (THIn) is proposed and utilized in this study to identify the temperature change hotspots, that is, the places with the most pronounced and robust exposure to temperature changes in the future across the Indian mainland. This multimodel multiscenario analysis is carried out using bias-corrected future-simulated temperature data from 14 state-of-the-art GCMs, participating in CMIP6, under two possible climate change scenarios—SSP245 and SSP585. Moreover, an in-depth spatiotemporal analysis of the future-projected temperature (maximum, minimum and average) is also carried out to understand the underlying mechanisms of these hotspot regions. Overall, the key findings of this study are listed below.

1. In general, a warmer future is expected over the Indian mainland with approximately $1.92 \pm 0.36^{\circ}C$ (SSP245) to $3.34 \pm 0.56^{\circ}C$ (SSP585) increase in average annual temperature w.r.t. the base period 1981–2010 across various models—which is much higher than the international target of 1.5 or $2^{\circ}C$ above the pre-industrial level towards the end of this century.
2. However, this unequivocal pattern of rising temperature is not spread uniformly across India. Places like north, central, western and J&K portion of India project as high as $\sim 4^{\circ}C$ increase in annual average temperature, whereas the eastern and southern parts of the country exhibits comparatively smaller increase ($<3^{\circ}C$). Similar increasing spatiotemporal pattern is reported for the extreme (95th percentile) temperature as well, which can be even more crucial considering its potentially detrimental effects on society.
3. Increase in average temperature is mostly dominated by the increase in minimum temperature, as compared to the increase in maximum temperature—holds true for all seasons. Such warming pattern remains persistent throughout the future and gets more intense with time, particularly under the higher emission scenario—indicating a potential impact of increased anthropogenic activities.
4. Overall, based on these future projected changes in various attributes of average temperature, such as mean, variability and extremes (magnitude, frequency and severity), the THIn is evaluated and accordingly entire Indian mainland is categorized into four zones of varying susceptibility—red, orange, yellow and green. Out of these four colour-coded regions, the red- and orange-coloured zones together are identified as temperature-based hotspots.
5. Region-wise analysis reveals that west, north, and J&K regions of India are most extensively occupied by the temperature changes hotspots, followed by north-east India. More than half of their areal extent is exposed to high to severe changes in temperature over future. On the other hand, southern and eastern part of India are projected to have the lowest share (even less than 10% of their area) of temperature-based hotspots.

Overall, the future-projected warming scenario over India is indeed alarming, which again underlines the necessity of suitable adaptation and mitigation strategies in sufficient advance, particularly for a developing country like India. We expect the findings of this study including the temperature-based colour-coded hotspot map for India will serve as a useful piece of information for the end users, as well as policymakers, to plan suitable region-specific management and adaptation strategies to combat the worst-case climate change scenario.

AUTHOR CONTRIBUTIONS

Subharthi Sarkar: Writing – original draft; investigation; formal analysis; methodology; data curation; software. **Rajib Maity:** Funding acquisition; supervision; writing – review and editing; conceptualization; resources; investigation; methodology.

ACKNOWLEDGEMENTS

This study is supported by a sponsored project supported by Ministry of Earth Science (MoES), Govt. of India, through a sponsored project (Grant No. MoES/PAMC/H&C/124/2019-PC-II). Authors further acknowledge the National Supercomputing Mission (NSM) for providing computing resources of "PARAM Shakti" at IIT Kharagpur, which is implemented by C-DAC and supported by the Ministry of Electronics and Information Technology (MeitY) and Department of Science and Technology (DST), Government of India. Finally, the authors thank the editors and anonymous reviewers whose constructive comments immensely improved the manuscript.

CONFLICT OF INTEREST STATEMENT

The authors declare no conflicts of interest.

DATA AVAILABILITY STATEMENT

The daily gridded observed maximum temperature data set for entire Indian mainland is obtained from of the India Meteorological Department (IMD), as mentioned in the in-text data citation reference Srivastava et al. (2009) and also can be freely accessed online via https://www.imdpune.gov.in/lrfindex.php. The simulated future daily maximum temperature datasets (2021–2100) are obtained from 14 state-of-the-art GCMs from the Earth System Grid Federation (ESGF) Archive under the auspices of the World Climate Research Programme (WCRP), that is, https://esgf-node.llnl.gov/search/cmip6/. All the figures in this manuscript are prepared using either MATLAB software (version R2021a, https://in.mathworks.com) or Microsoft EXCEL 2016.

ORCID

Subharthi Sarkar https://orcid.org/0000-0002-8273-7668

Rajib Maity https://orcid.org/0000-0001-5631-9553

ENDNOTE

[1] In order to maintain consistency in the analysis, data from all 14 GCMs are obtained for the "r1i1p1f1" variant level, which stands for the ensemble combination of 1st realization (*r*), 1st initialization (*i*), 1st physics (*p*) and 1st forcing (*f*).

REFERENCES

Aggarwal, P. (2022) Devastating heatwaves in India: Here's all you need to know. *India Today*. New Delhi, 15 June. Available from: https://www.indiatoday.in/diu/story/devastating-heatwaves-in-india-all-you-need-to-know-1962392-2022-06-14

Ashfaq, M., Rastogi, D., Mei, R., Touma, D. & Ruby, L.L. (2017) Sources of errors in the simulation of South Asian summer monsoon in the CMIP5 GCMs. *Climate Dynamics*, 49(1–2), 193–223. Available from: https://doi.org/10.1007/s00382-016-3337-7

Basha, G., Kishore, P., Ratnam, M.V., Jayaraman, A., Kouchak, A.A., Ouarda, T.B.M.J. et al. (2017) Historical and projected surface temperature over India during the 20th and 21st century. *Scientific Reports*, 7(1), 1–10. Available from: https://doi.org/10.1038/s41598-017-02130-3

Basu, J. (2022) Unprecedented early heatwaves in India, Pakistan 30 times more likely in 2022 due to climate change: scientists. *Down to Earth*, 25 May. Available from: https://www.downtoearth.org.in/news/climate-change/state-of-india-s-environment-in-figures-india-recorded-280-heat-wave-days-across-16-states-in-2022-most-in-decade-83131

Chen, C.A., Hsu, H.H. & Liang, H.C. (2021) Evaluation and comparison of CMIP6 and CMIP5 model performance in simulating the seasonal extreme precipitation in the Western North Pacific and East Asia. *Weather and Climate Extremes*, 31, 100303. Available from: https://doi.org/10.1016/j.wace.2021.100303

Dash, S.K., Jenamani, R.K. & Mohapatra, M. (2022) India's prolonged heatwave linked to record poor summer rains. *Nature India*. Available from: https://www.nature.com/articles/d44151-022-00054-0

De Souza, K., Kituyi, E., Harvey, B., Leone, M., Murali, K.S. & Ford, J.D. (2015) Vulnerability to climate change in three hot spots in Africa and Asia: key issues for policy-relevant adaptation and resilience-building research. *Regional Environmental Change*, 15(5), 747–753. Available from: https://doi.org/10.1007/s10113-015-0755-8

Di Luca, A., Pitman, A.J. & de Elía, R. (2020) Decomposing temperature extremes errors in CMIP5 and CMIP6 models. *Geophysical Research Letters*, 47(14), e2020GL088031. Available from: https://doi.org/10.1029/2020GL088031

Diffenbaugh, N.S. & Barnes, E.A. (2023) Data-driven predictions of the time remaining until critical global warming thresholds are reached. *Proceedings of the National Academy of Sciences of the United States of America*, 120(6), 1–9.

Diffenbaugh, N.S. & Giorgi, F. (2012) Climate change hotspots in the CMIP5 global climate model ensemble. *Climatic Change*, 114(3–4), 813–822. Available from: https://doi.org/10.1007/s10584-012-0570-x

Gidden, M.J., Riahi, K., Smith, S.J., Fujimori, S., Luderer, G., Kriegler, E. et al. (2019) Global emissions pathways under different socioeconomic scenarios for use in CMIP6: a dataset of harmonized emissions trajectories through the end of the century. *Geoscientific Model Development*, 12(4), 1443–1475. Available from: https://doi.org/10.5194/gmd-12-1443-2019

Gudmundsson, L., Bremnes, J.B., Haugen, J.E. & Engen-Skaugen, T. (2012) Technical note: downscaling RCM precipitation to the station scale using statistical transformations—a comparison of methods. *Hydrology and Earth System Sciences*, 16(9), 3383–3390. Available from: https://doi.org/10.5194/hess-16-3383-2012

IMD. (2022) *Statement on climate of India during 2022*. Pune: IMD. Available from: https://mausam.imd.gov.in/Forecast/marquee_data/Statement_climate_of_india_2022_final.pdf

IPCC. (2021) *Summary for policymakers. Climate change 2021: the physical science basis. Contribution of Working Group I to the sixth assessment report of the Intergovernmental Panel on Climate Change*. Cambridge and New York, NY: Cambridge University Press.

Kishore, P., Jyothi, S., Basha, G., Rao, S.V.B., Rajeevan, M., Velicogna, I. et al. (2015) Precipitation climatology over India: validation with observations and reanalysis datasets and spatial trends. *Climate Dynamics*, 46(1–2), 541–556.

Knutti, R., Rogelj, J., Sedlácek, J. & Fischer, E.M. (2016) A scientific critique of the two-degree climate change target. *Nature Geoscience*, 9(1), 13–18. Available from: https://doi.org/10.1038/ngeo2595

Kotharkar, R. & Ghosh, A. (2021) Review of heat wave studies and related urban policies in South Asia. *Urban Climate*, 36, 100777. Available from: https://doi.org/10.1016/j.uclim.2021.100777

Li, J., Huo, R., Chen, H., Zhao, Y. & Zhao, T. (2021) Comparative assessment and future prediction using CMIP6 and CMIP5 for annual precipitation and extreme precipitation simulation. *Frontiers in Earth Science*, 9, 1–20. Available from: https://doi.org/10.3389/feart.2021.687976

Luan, G., Yin, P., Wang, L. & Zhou, M. (2019) Association between ambient temperature and chronic obstructive pulmonary disease: a population-based study of the years of life lost. *International Journal of Environmental Health Research*, 29(3), 246–254. Available from: https://doi.org/10.1080/09603123.2018.1533533

Mani, M., Bandyopadhyay, S., Chonabayashi, S., Markandya, A. & Mosier, T. (2018) *South Asia's hotspots and precipitations: the impact of temperature and precipitation changes on living standards. South Asia development matters*. Washington, DC: World Bank.

Mishra, V., Bhatia, U. & Tiwari, A.D. (2020) Bias-corrected climate projections for South Asia from Coupled Model Intercomparison Project-6. *Scientific Data*, 7(1), 1–13. Available from: https://doi.org/10.1038/s41597-020-00681-1

Mishra, V., Kumar, D., Ganguly, A.R., Sanjay, J., Mujumdar, M., Krishnan, R. et al. (2014) Reliability of regional and global climate models to simulate precipitation extremes over India. *Journal of Geophysical Research: Atmospheres*, 119, 9301–9323.

Mishra, V., Mukherjee, S., Kumar, R. & Stone, D.A. (2017) Heat wave exposure in India in current, 1.5°C, and 2.0°C worlds. *Environmental Research Letters*, 12(12), 124012. Available from: https://doi.org/10.1088/1748-9326/aa9388

Nandi, S. & Swain, S. (2022) Analysis of heatwave characteristics under climate change over three highly populated cities of South India: a CMIP6-based assessment. *Environmental Science and Pollution Research*, 30(44), 99013–99025. Available from: https://doi.org/10.1007/s11356-022-22398-x

Pascal, M., Wagner, V., Alari, A., Corso, M. & Le Tertre, A. (2021) Extreme heat and acute air pollution episodes: a need for joint public health warnings? *Atmospheric Environment*, 249, 118249. Available from: https://doi.org/10.1016/j.atmosenv.2021.118249

Piani, C., Haerter, J.O. & Coppola, E. (2010) Statistical bias correction for daily precipitation in regional climate models over Europe. *Theoretical and Applied Climatology*, 99(1–2), 187–192. Available from: https://doi.org/10.1007/s00704-009-0134-9

Rao, K.K., Jyoteeshkumar Reddy, P. & Chowdary, J.S. (2023) Indian heatwaves in a future climate with varying hazard thresholds. *Environmental Research: Climate*, 2(1), 015002. Available from: https://doi.org/10.1088/2752-5295/acb077

Ray, K., Giri, R.K., Ray, S.S., Dimri, A.P. & Rajeevan, M. (2021) An assessment of long-term changes in mortalities due to extreme weather events in India: a study of 50 years' data, 1970–2019. *Weather and Climate Extremes*, 32, 100315. Available from: https://doi.org/10.1016/j.wace.2021.100315

Roe, S., Streck, C., Obersteiner, M., Frank, S., Griscom, B., Drouet, L. et al. (2019) Contribution of the land sector to a 1.5°C world. *Nature Climate Change*, 9(11), 817–828. Available from: https://doi.org/10.1038/s41558-019-0591-9

Rogelj, J., Den Elzen, M., Höhne, N., Fransen, T., Fekete, H., Winkler, H. et al. (2016) Paris Agreement climate proposals need a boost to keep warming well below 2°C. *Nature*, 534(7609), 631–639. Available from: https://doi.org/10.1038/nature18307

Rohini, P., Rajeevan, M. & Mukhopadhay, P. (2019) Future projections of heat waves over India from CMIP5 models. *Climate Dynamics*, 53(1), 975–988. Available from: https://doi.org/10.1007/s00382-019-04700-9

Romanello, M., Di Napoli, C., Drummond, P., Green, C., Kennard, H., Lampard, P. et al. (2022) The 2022 report of the Lancet Countdown on health and climate change: health at the mercy of fossil fuels. *Lancet*, 400(10363), 1619–1654. Available from: https://doi.org/10.1016/S0140-6736(22)01540-9

Salunke, P., Keshri, N.P., Mishra, S.K. & Dash, S.K. (2023) Future projections of seasonal temperature and precipitation for India. *Frontiers in Climate*, 5, 1069994. Available from: https://doi.org/10.3389/fclim.2023.1069994

Sarkar, S., Maity, S.S. & Maity, R. (2023) Precipitation-based climate change hotspots across India through a multi-model assessment from CMIP6. *Journal of Hydrology*, 623, 129805. Available from: https://doi.org/10.1016/j.jhydrol.2023.129805

Sen, P.K. (1968) Estimates of the regression coefficient based on Kendall's tau. *Journal of the American Statistical Association*, 63(324), 1379–1389. Available from: https://doi.org/10.1080/01621459.1968.10480934

Seneviratne, S.I., Nicholls, N., Easterling, D., Goodess, C.M., Kanae, S., Kossin, J. et al. (2012) Changes in climate extremes and their impacts on the natural physical environment. In: *Managing the risks of extreme events and disasters to advance climate change adaptation: a special report of Working Groups I and II of the Intergovernmental Panel on Climate Change (IPCC)*. Cambridge and New York, NY: Cambridge University Press, pp. 109–230.

Sharma, S. & Mujumdar, P. (2017) Increasing frequency and spatial extent of concurrent meteorological droughts and heatwaves in India. *Scientific Reports*, 7(1), 1–9. Available from: https://doi.org/10.1038/s41598-017-15896-3

Singh, S., Mall, R.K. & Singh, N. (2021) Changing spatio-temporal trends of heat wave and severe heat wave events over India: an emerging health hazard. *International Journal of Climatology*, 41(S1), E1831–E1845. Available from: https://doi.org/10.1002/joc.6814

Smith, D.M., Scaife, A.A., Hawkins, E., Bilbao, R., Boer, G.J., Caian, M. et al. (2018) Predicted chance that global warming will temporarily exceed 1.5°C. *Geophysical Research Letters*, 45(21), 11895–11903. Available from: https://doi.org/10.1029/2018GL079362

Srivastava, A.K., Kothawale, D.R. & Rajeevan, M.N. (2017) Variability and long-term changes in surface air temperatures over the Indian subcontinent. In: Rajeevan, M.N. & Nayak, S. (Eds.) *Observed climate variability and change over the Indian region. Springer geology*. Singapore: Springer, pp. 17–35.

Srivastava, A.K., Rajeevan, M. & Kshirsagar, S.R. (2009) Development of a high resolution daily gridded temperature data set

(1969–2005) for the Indian region. *Atmospheric Science Letters*, 10, 249–254. Available from: https://doi.org/10.1002/asl.232

Supharatid, S., Nafung, J. & Aribarg, T. (2021) Projected changes in temperature and precipitation over mainland Southeast Asia by CMIP6 models. *Journal of Water and Climate Change*, 13, 337–356. Available from: https://doi.org/10.2166/wcc.2021.015

Taylor, K.E., Stouffer, R.J. & Meehl, G.A. (2012) An overview of CMIP5 and the experiment design. *Bulletin of the American Meteorological Society*, 93(4), 485–498. Available from: https://doi.org/10.1175/BAMS-D-11-00094.1

Trenberth, K.E. (2011) Changes in precipitation with climate change. *Climate Research*, 47(1–2), 123–138. Available from: https://doi.org/10.3354/cr00953

Turco, M., Palazzi, E., Von Hardenberg, J. & Provenzale, A. (2015) Observed climate change hotspots. *Geophysical Research Letters*, 42(9), 3521–3528. Available from: https://doi.org/10.1002/2015GL063891

UNFCCC. (2015) *Adoption of the Paris Agreement FCCC/CP/2015/-L.9/Rev.1*. Paris: United Nations Framework Convention on Climate Change.

Wang, D., Liu, J., Shao, W., Mei, C., Su, X. & Wang, H. (2021) Comparison of CMIP5 and CMIP6 multi-model ensemble for precipitation downscaling results and observational data: the case of Hanjiang River basin. *Atmosphere*, 12(7), 867. Available from: https://doi.org/10.3390/atmos12070867

Wasko, C. (2021) Review: Can temperature be used to inform changes to flood extremes with global warming? *Philosophical Transactions of the Royal Society A: Mathematical, Physical and Engineering Sciences*, 379(2195), 20190551. Available from: https://doi.org/10.1098/rsta.2019.0551

Yu, B., Wang, X.L., Feng, Y., Chan, R., Compo, G.P., Slivinski, L.C. et al. (2022) Northern Hemisphere extratropical cyclone activity in the twentieth century reanalysis version 3 (20CRv3) and its relationship with continental extreme temperatures. *Atmosphere*, 13(8), 1166. Available from: https://doi.org/10.3390/atmos13081166

Zhang, Y., Feng, R., Wu, R., Zhong, P., Tan, X., Wu, K. et al. (2017) Global climate change: impact of heat waves under different definitions on daily mortality in Wuhan, China. *Global Health Research and Policy*, 2(1), 1–9. Available from: https://doi.org/10.1186/s41256-017-0030-2

SUPPORTING INFORMATION

Additional supporting information can be found online in the Supporting Information section at the end of this article.

How to cite this article: Sarkar, S., & Maity, R. (2024). Unveiling climate change-induced temperature-based hotspots across India through multimodel future analysis from CMIP6. *International Journal of Climatology*, *44*(2), 627–646. https://doi.org/10.1002/joc.8348